Journal of Sustainability Science and Management
Volume 19 Number 12, December 2024: 120-140
eISSN: 2672-7226

SYNTHESIS OF NANOCELLULOSE USING ULTRASOUND - ASSISTED ACID HYDROLYSIS FOR ADSORPTION/OXIDATION OF ORGANIC POLLUTANTS IN WASTEWATER UNDER UV AND SOLAR LIGHT

ALI ABD HASSAN[1,2,3]* AND IBTEHAL KAREEM SHAKIR[3]

[1]Chemical Engineering Department, College of Engineering, Al-Muthanna University, 87QQ+3VG, Samawah, Al-Muthanna, Iraq. [2]Petroleum Department, College of Engineering, AL-Ayen University, Thi-Qar, Iraq. [3]Chemical Engineering Department, College of Engineering, University of Baghdad, Baghdad, Iraq.

**Corresponding author: ali.alkhafaji@mu.edu.iq.*
http://doi.org/10.46754/jssm.2024.12.008
Received: 8 July 2024 *Accepted: 2 September 2024* *Published: 15 December 2024*

Abstract: This work aimed to prepare nanocrystals of cellulose (NCW) through hydrolysis of Cotton Waste (CW) by nitric acid assisted with ultrasound/high temperature under optimum conditions. The synthesised NCW was thoroughly characterised using various techniques, including FTIR for surface functional groups analysis, FE-SEM, EDX, DRS, BET, and XRD for structural characterisation. Thermogravimetric analysis was utilised to investigate the thermal properties of NCW. The XRD data revealed a crystallite size of 10 nm to 50 nm while the average particle size from FE-SEM was calculated by ImageJ software. The hydrolysis and sonication treatment resulted in cellulose nanoparticles with irregular morphology with average particle sizes of 110 nm and less than 200 nm, respectively. The NCW particles obtained showed potential for the removal of organic pollutants in water treatment applications. Organic removal ratios of 92.5% and 82.3% were achieved for nanocellulose used as adsorbent and oxidant under UV and solar light.

Keywords: Cotton waste, nanocellulose, water treatment, adsorbent, optimisation.

Introduction

Nanocellulose is a cutting-edge natural polymer extracted from cellulose found in plants and bacteria. This micro/nano family cellulose includes nanocrystalline cellulose, nano whiskers, cellulose nanofibrils, microfibrillated cellulose, and bacterial cellulose, also known as microbial cellulose (Mondal *et al*., 2023). These materials are sourced from various natural sources such as wood, cotton, hemp, jute, sugar cane, wheat straw, algae, and tunicin, among others (Jayasinghe *et al*., 2020). The burgeoning interest in nanotechnology and nanomaterials has sparked extensive research in cellulosic nanomaterials (Nawaf *et al*., 2019).

As particle sizes decrease toward the atomic scale, materials undergo alterations or enhancements in their properties, often exhibiting new capabilities or improvements for novel value-added materials (Amelia *et al*., 2024). Cellulose, in particular, has garnered attention for its ability to form a three-dimensional nonporous fibre network with fibre diameters typically ranging from 30 nm to 50 nm —much thinner than plant cellulose. Among the various types of nanocellulose, NCW are particularly common and are typically prepared using acid hydrolysis methods. NCW is often stored in the form of aqueous suspension due to the abundance of hydrophilic groups on its surface (Abdullah *et al*., 2024).

Many cellulose-rich materials have served as a raw source for the synthesis of cellulose nanocrystals. Among them, cotton stands out as a promising reserve due to its high cellulose content exceeding 90%, coupled with its abundant availability (Négrier *et al*., 2023). Furthermore, cotton waste and products of cotton can also be repurposed for NCW preparation, presenting a sustainable approach to vaporise cotton resources (Mohana *et al*., 2023). The production of NCW from cotton waste represents a promising method of resource reutilisation. NCW derived from cotton exhibits competitive physicochemical properties and is cost-effective (Tan *et al*., 2023). Cellulose, renowned for its exceptional surface and structural properties is

undergoing extensive research across various domains. Its applications span a wide range of industries, including food, chemicals, textiles, biomaterials, electronics, electrochemical devices, pharmaceuticals, and more. In this context, both cotton and its waste hold significant potential for the production of valuable products such as ethanol, biogas, organic acids, cellulose powders, and cellulose nanoparticles (Liu *et al*., 2021). Nonetheless, large-scale industrialisation remains challenging, chiefly due to the requisite raw material retreatment and the high cost associated with cellulose extraction.

Presently, prevalent methods for nanocellulose preparation encompass the use of sulfuric acid, hydrochloric acid, nitric acid hydrolysis, TEMPO oxidation, mechanical techniques, biological enzyme processes, and steam explosion methodologies. However, each method has limitations. For instance, TEMPO reagent usage is costly and challenging to recover, resulting in substantial wastewater production. Mechanical and explosive methods necessitate specialised equipment with high energy consumption but yielding low-purity products (Kryeziu *et al*., 2022).

While the biological approach aligns with green and sustainable principles, its efficiency is hampered by stringent reaction conditions, impeding large-scale implementation. In contrast, acid hydrolysis stands out for its simplicity and maturity (Shi *et al*., 2022). Dating back to 1947, studies have explored cellulose hydrolysis with sulfuric acid to produce NCWs. Notably, this method generates degraded sugar by-products that can be further fermented into biofuel. Moreover, acid recovery is feasible, enhancing its economic viability. Consequently, acid hydrolysis remains the predominant technique for the rapid production of nanocellulose (Yu *et al*., 2021).

Nowadays, wastewater treatment has garnered significant importance due to the considerable discharge of organic pollutants (S. Raheem *et al*., 2024). Organic pollutants are chemicals that are carbon-based and can be harmful to the environment and human health such as phenol, benzene, gas, and aromatics. This influx of pollutants into water bodies poses a severe threat to aquatic ecosystems, precipitating a decline in living standards and environmental quality (Ibrahim *et al*., 2019). To address this pressing issue, various methods have been employed, including physical, chemical, and biological approaches (AlJaberi *et al*., 2020). However, these methods are beset by limitations such as the persistence of refractory organic wastewater and high equipment costs (Rashid *et al*., 2020). Consequently, the quest for an efficient and cost-effective wastewater treatment method persists as a significant challenge.

In recent years, the utilisation of adsorbents has emerged as a straightforward, efficient, economical, and environmentally friendly approach for water purification (Al-Zobai & Hassan, 2022; Nawaf *et al*., 2023). Adsorbents offer the advantage of selectively removing contaminants from water, thereby improving water quality and mitigating environmental degradation (Maiti *et al*., 2017; Nawaf *et al*., 2021). Hence, bio-based chemicals and materials derived from cellulose hold promise for diverse applications (Al-Jubouri *et al*., 2019). Research efforts have increasingly focused on exploring the potential of bio-based materials derived from cellulose (Qureshi *et al*., 2020) with the added advantage of the adsorbent's potential for reuse through appropriate desorption and regeneration processes. While, activated carbon adsorbents have traditionally been used for this purpose because of their high surface area and large pore volume, cellulose offers distinct compositions, structures, and properties (Wang & Lu, 2020).

In contrast, Advanced Oxidation Processes (AOPs) offer an efficient alternative for water purification. By generating oxidising radicals like free radicals, AOPs enable the total mineralisation of pollutants or the formation of less toxic compounds. Free radicals possess a high oxidation potential and can effectively oxidise recalcitrant organic pollutants (Nsaif *et al*., 2023). Photochemical initiation is a valuable technique for introducing various vinyl monomers onto cellulose materials (Alamery

& Hassan, 2022). When exposed to ultraviolet light, a sensitiser, monomer, polymer, or excited cellulose molecule absorbs energy, leading to the dissociation of the excited molecule into reactive free radicals that initiate the grafting process (Hassan *et al*., 2022). Taking consideration of this work, NCW derived from cotton waste via acid hydrolysis, assisted by ultrasounds under high temperature, yields a novel nanocellulose with unique properties and applications. The synthesised nanocellulose was utilised for both adsorption and UV or solar light degradation of organic content in refinery wastewater. Through systematic investigation of experimental parameters such as dosage, pH, temperature, and reaction time, the adsorption and solar catalytic degradation processes were optimised.

Materials and Methods

Chemical and Analytical Analysis

Refinery wastewater (RWW) contaminated with organic pollutants was obtained from the discharge of an oilfield refinery. RWW was stored at 5°C in a polypropylene container. The specifications of the RWW are listed in Table 1. All materials used in this study were of analytical grade and underwent no additional purification. Cotton waste was sourced from tailoring workshops, were cut, and shredded. Chemicals such as H_2SO_4 (SDFCL, 98% purity), nitric acid, acetic acid, sodium chloride, carbon tetrachloride, hydrogen peroxide, and sodium hydroxide (Thomas Baker) were utilised. After each experiment, 0.2 g of sodium chloride was added to 40 mL of RWW in a separating funnel to disrupt the organic emulsion. Subsequently, 4 mL of carbon tetrachloride was added and vigorously shaken for two minutes. After a further 20 minutes, once the solution had separated into two distinct layers, the lower (organic) layer was determined using a UV-1800 spectrophotometer (UV-1800 Shimadzu, Japan) (Naser *et al*., 2021).

The organic elimination efficacy was assessed by Equation (1):

$$Y_{OCRE} = \frac{B_o - B_t}{B_o} \times 100\% \quad (1)$$

where B_o and B_t are the concentrations of organic (mg/L) before and after treatment.

The Preparation of NCW

The cotton waste was washed with cold and hot water consecutively until a constant colouration was visually observed. Next, in the steps of washing, CW was added to a 5% NaOH solution and stirred continuously according to the lecture by Theivasanthi *et al*. (2018). The CW treated with sodium hydroxide was then cleaned and washed numerous times with distilled water to reach a natural pH to eliminate hemicellulose and lignin. The CW with NaOH was then desiccated at 75°C in an oven for 24 hours to produce NaOH/CW. Next, the alkali-treated cotton waste was added to a solution containing 2% acetic acid and 7% hydrogen peroxide (Zang & Qian, 2012). The alkali-treated cotton was impregnated in the solution of 10/20 mL concentrated nitric acid and distilled water, heated at 50°C with constant stirring for two hours to ensure thorough hydrolysis under ultrasounds and UV light. The resulting mixture was washed several times with water until a neutral pH was achieved. Figure 1 illustrates

Table 1: Specification of refinery wastewater

Limits	Values	Limits	Values
Oil content	165.3 mg/L	Conductivity	510,000 µs/cm
Turbidity	24.79 NTU	TDS	326,400 mg/L
pH	7.1	Viscosity	1.0103 m Pa/S
Solution oxygen content	0.032 mg/L	Iron	0.21 mg/L
Specific gravity	0.9965	Sulphate	55.2 mg/L

this process while Figure 2 depicts the step-by-step extraction of NCW from the cotton waste. Initially, the cotton waste was bleached using H_2O_2, followed by nitric acid hydrolysis in the presence of ultrasound under UV light, as described in the procedure by Pandi *et al*. (2021a) by using nitric acid under UV light at high temperature.

Characterisation

Fourier-transform infrared spectroscopy (FTIR) was employed using Attenuated Total Reflectance (ATR) mode to analyse the functional groups present in the composite adsorbent. FTIR spectroscopy provides information about chemical bonds and molecular structure in the range of 4,000 to 400 cm^{-1}. Field Emission Scanning Electron Microscopes (FE-SEM) were utilised to examine the surface morphology and structure of both the raw CW and the composite adsorbent. XRD provides information about the crystalline structure and phase composition of the materials. A TGA analyser (TA Instruments Q-500) was employed at an air atmosphere at a heating rate of 10°C per minute from ambient temperature to 600°C. EDX is used in combination with FE-SEM to analyse the elemental composition of the composite materials. UV-visible diffuse reflectance spectroscopy is employed

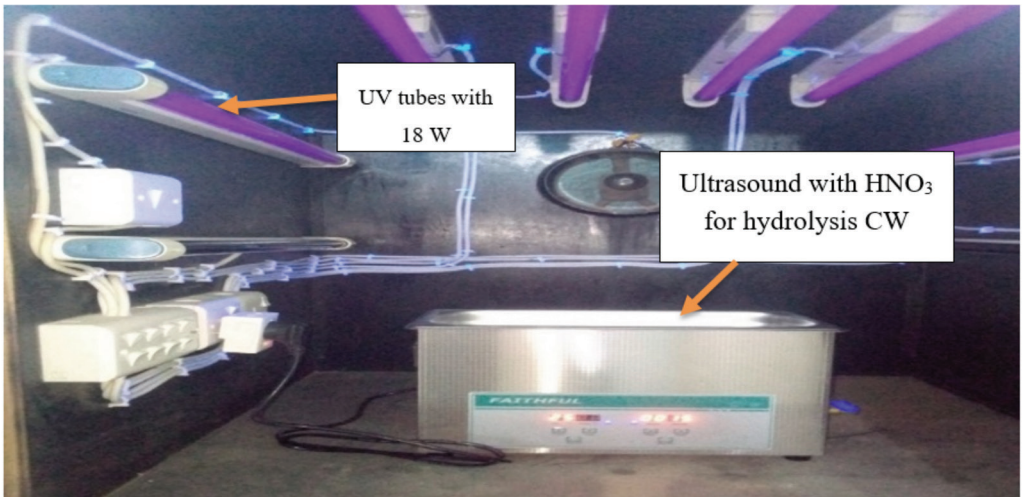

Figure 1: The preparation of NCW

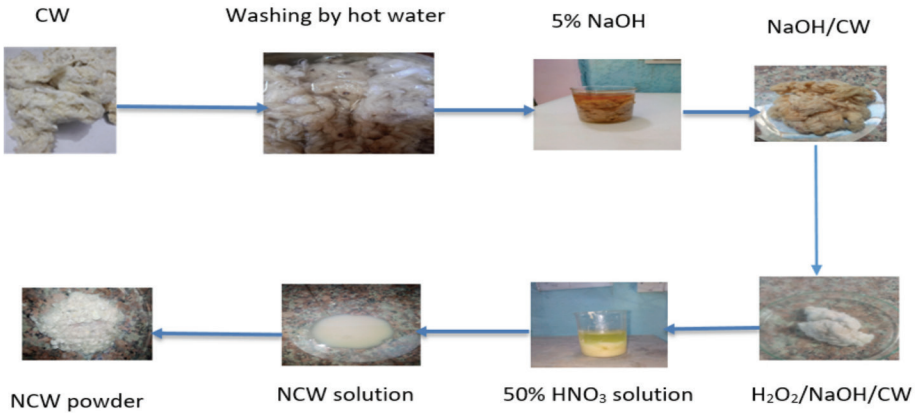

Figure 2: Scheme explanation of NCW

to evaluate the energy band gap (Eg) of the semiconductor nanostructures. Surface area and pore volume measurements were carried out using the Brunauer, Emmett, and Teller (BET) method with a Thermo Analyser (Thermo Fisher Scientific, United States).

Batch Adsorption/Photodegradation Treatment

The adsorption/degradation experiments were shown in a magnetic model batch reactor, which contained 150 mL of refinery wastewater in a box chamber with eight UV lamps, each with a power output of 18 W and a wavelength of 365 nm. A magnetic stirrer was used to ensure thorough mixing of RWW within the reactor. Before the addition of the NCW dose, the pH was adjusted utilising a dilute NaOH or H_2SO_4 solution. The pH of wastewater is vital as it can impact the capacity of adsorption and competence of the treatment process. The intensity of the UV light was maintained at 0.5 mW/cm^2 for the best conditions for a degradation reaction. Solar degradation tests were also conducted by employing natural sunlight. The set up comprised the adsorbent material used for organic elimination and a photo chamber, where the degradation process takes place. The photo chamber is equipped with UV lamps or designed to use natural sunlight for light-driven degradation reactions. Figure 3 (A) and (B) depict the set up for UV light and solar degradation processes, respectively.

Experimental Design

This study aimed to optimise conditions for the mineralisation and treatment of organic pollutants from RWW utilising nanocrystalline cellulose from CW. The Box-Bingham Design (BBD) technique, coupled with Response Surface Methodology (RSM) was employed for this purpose. Experimental design, statistical analysis, and graphical representation were conducted using Design Expert Minitab-17 software. The independent variables considered in the experimental design were oxidation time (X_1), pH (X_2), dose (X_3), and temperature (X_4). These variables were coded at low and high levels within the Box-Bingham Design, as outlined in Table 2.

Table 2: Operational parameters

Parameters	Ranges
X_1: Oxidation time (minute)	30-120
X_2: pH	3-9
X_3: Adsorbent (gm)	0.5-1
X_4: Temperature (°C)	25-70

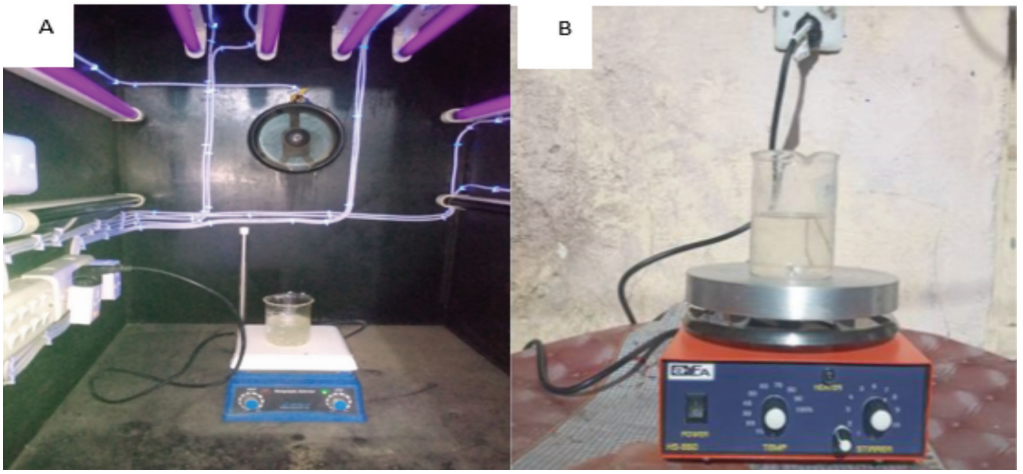

Figure 3: (A) and (B) are the set up for UV and solar degradation processes

Results and Discussion

The Characteristics of NCW

Figure 4 illustrates the FTIR analysis of untreated cotton waste, cotton hydrolysed by nitric acid, and the corresponding nanoparticles of cellulose. Similar spectra were observed for all samples, showcasing characteristic peaks indicative of the crystalline Iβ structure (Raheem *et al*., 2024). Notably, the OH stretching at 3,265 cm^{-1} and OH out of plane winding at 720 cm^{-1} were retained after hydrolysis and ultrasonication under UV light.

Several characteristic peaks were observed in cotton, including those at 3,800-3,002, 2,901, 1,640, 1,430, 1,374, 1,164, and 897 cm^{-1}. The band at 3,810-3,005 cm^{-1} corresponds to the stretching of OH and flexural vibration of intra- and intermolecular hydrogen bonds of cellulose. Changes in the quantity and quality of hydrogen bonds led to variations in the intensity and width of this band. The vibrations at 2,904 and 2,855 cm^{-1} are credited to CH_2 unequal vibrations, though the peak at 1,630 cm^{-1} is related to the OH bending of nanocellulose wetness. This peak was strongly aimed at the NCW owing to their larger surface area compared to untreated and hydrolysed CW (Mirzaei, 2021).

The band at 1,430 cm^{-1} is linked to the HCH and OCH in-plane meandering vibrations and is carefully a crystalline absorption band. Moreover, the vibration at 1,374 cm^{-1} corresponds to CH distortion vibration and the band at 1,164 cm^{-1} is attributed to unequal bridge oxygen stretching vibration (i.e., of C_1-O-C_4 groups). Also, the band at 897 cm^{-1}, chosen as an amorphous absorption band is connected to COC, CCO, and CCH deformation modes and stretching vibrations of the C-5 and C-6 atoms. Overall, all bands retained their positions after hydrolysis and ultra sonication under UV light (Meyabadi *et al*., 2014).

Cellulose consists of both crystalline and amorphous regions with the percentage of the crystalline portion relative to the total cellulose is termed crystallinity. Understanding the crystallinity of NCW is crucial in cellulose research. In Figure 5, the diffraction peak of the 002 crystal plane of cellulose is observed near 22° (Al-Jubouri, 2019). Additionally, the Full Width at Half Maximum (FWHM) of all peaks, d-spacing, and crystallite size of NCWs were calculated and reported in Table 3. The crystallite size of NCWs was determined by employing the Scherrer formula, Equation (2).

$$D = \frac{K\lambda}{\beta \sin\sin \theta} \quad (2)$$

The crystallite size (D) is determined using the Scherrer formula, where K is Bragg's constant, β is the full width at half maximum, θ is

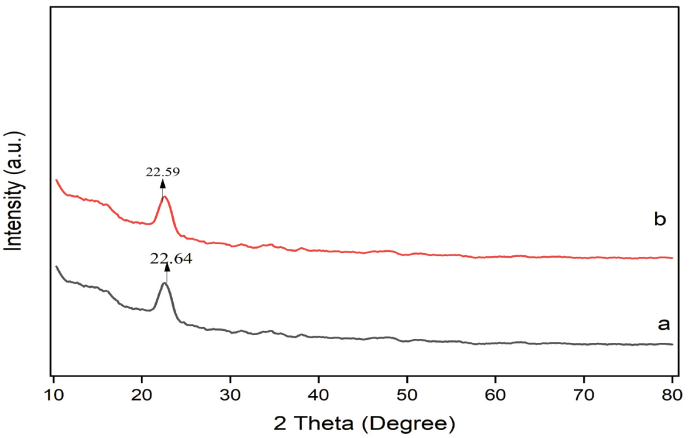

Figure 4: XRD patterns of (a) CW and (b) NCW adsorbent

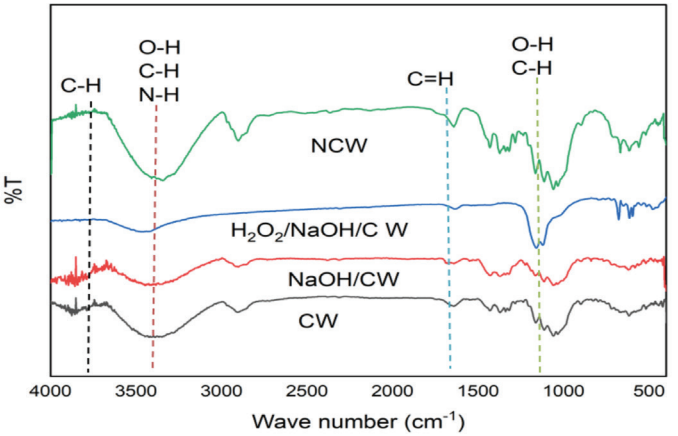

Figure 5: FTIR analysis CW, NaOH/CW, H_2O_2/NaOH/CW, and NCW adsorbent

Table 3: Structural parameters of NCW

No.	Pos. [°2 Th.]	Height [cts]	FWHM Left [°2 Th.]	d-spacing	Crystalline Size (nm)
1	22.59(2)	124(4)	1.36(5)	3.93349	100.00
2	22.64(2)	62(4)	1.36(5)	3.93349	50.00

the Bragg angle, and λ is the X-ray wavelength. In this study, the dominant (200) peak produced a crystallite size of 44.81 nm with a corresponding d-spacing of 3.93 Å. Comparing the crystallinity of NCWs synthesised in this work with those in previous literature, the obtained crystallinity was 6.326 nm (Kurniawan *et al*., 2023).

Figure 6 shows FE-SEM images of CW, NaOH/CW, and NCWs synthesised under various acid concentrations and ultrasound conditions. CW exhibits a smooth surface [Figures 6 (a) and (b)], whereas the bimetallic composite displays a polygonal and abrasive structure. The formation of binary and/or triple nanocomposites leads to the disappearance of some diffraction peaks of the individual components, indicating the formation of new phases or changes in the crystalline structure (Mahmood & Abid, 2020). However, major peaks of the individual components remain visible or slightly deviate from their original positions, suggesting that the nanocomposites retain some characteristics of their constituent materials. NCW nanoparticles are spherical, ranging in size from 50 nm to 150 nm with an average particle size of 110 nm, as depicted in Figure 7. The morphology of cotton waste aligns with previous descriptions (Alfattal & Abbas, 2019), providing validation and continuity in the characterisation process (Simayee *et al*., 2023).

EDX analysis was performed to evaluate the purity of CW and NCW, as illustrated in Figure 8. The analysis indicated the presence of carbon (C) and oxygen (O) elements in the samples, as outlined in Table 4. No impurity peaks were detected, indicating high sample purity and confirming the presence of the intended elements. Carbon was a major constituent of cellulose, forming the backbone of the polysaccharide structure and oxygen was present in hydroxyl groups (-OH), and ether linkages within the cellulose chains. Both are as described for pure cellulose (Mhawesh & Abd Ali, 2020). UV-DRS analysis was employed to determine the optical properties of the prepared catalyst and evaluate its capability to generate electron-hole pairs during the photodegradation process.

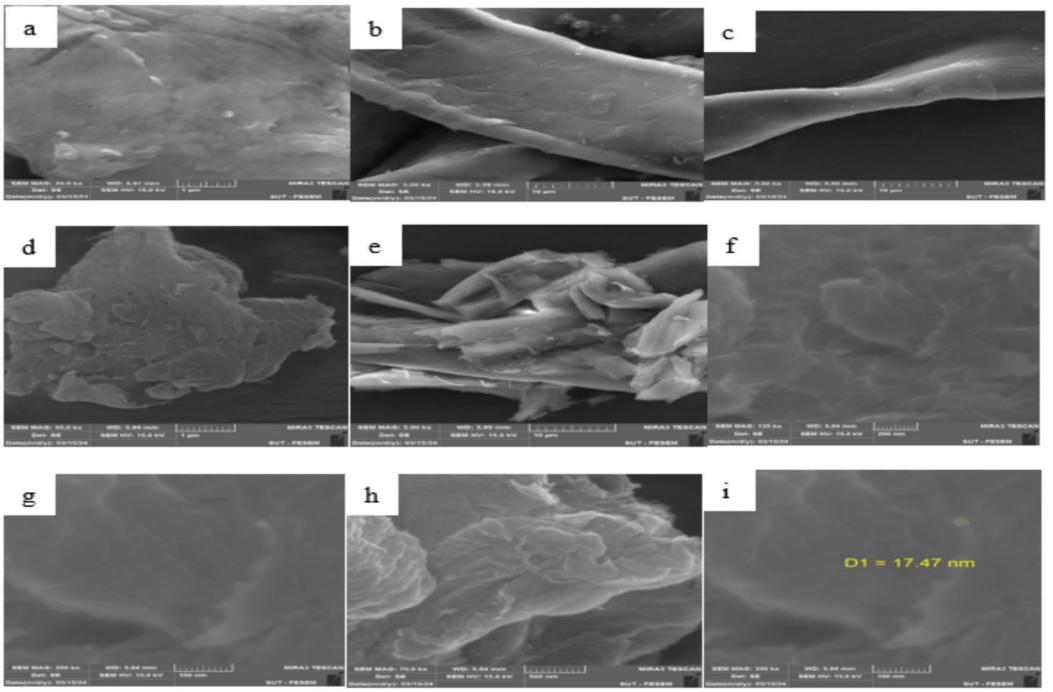

Figure 6: (a) CW at 1µm, (b) CW at 10µm, (c) NaOH/CW at 10µm, (d) NCW at 1µm, (e) NCW at 10 µm, (f) NCW at 200 nm, (g) NCW at 100 nm, (h) NCW at 500 nm, and (i) NCW at 100 nm

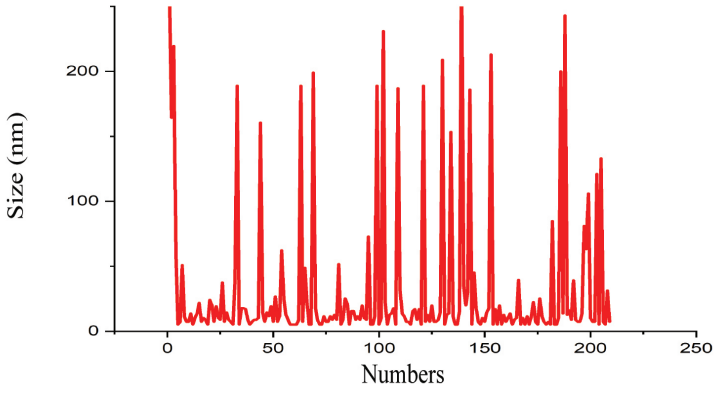

Figure 7: Particle size distribution of NCW

In Figure 9, the energy band gap (Eg) values of the synthesised NCW samples were measured to be 3.28 eV. The absorption peaks of the samples were observed within the range of 350 nm to 360 nm. The increased surface area of the nanorods and their uniform distribution on the cellulose surface may contribute to the enhanced UV absorption efficiency (Motlagh *et al*., 2023). TGA of the NCW are presented in Figure 10. TGA was conducted to analyse the thermal stability and weight loss of the samples as the temperature increased from 54°C to 600°C at a rate of 10°C per minute. An initial weight loss of 5.75% was observed below 200°C, attributed to the evaporation of volatile components present in NCWs and moisture. Subsequently, a major

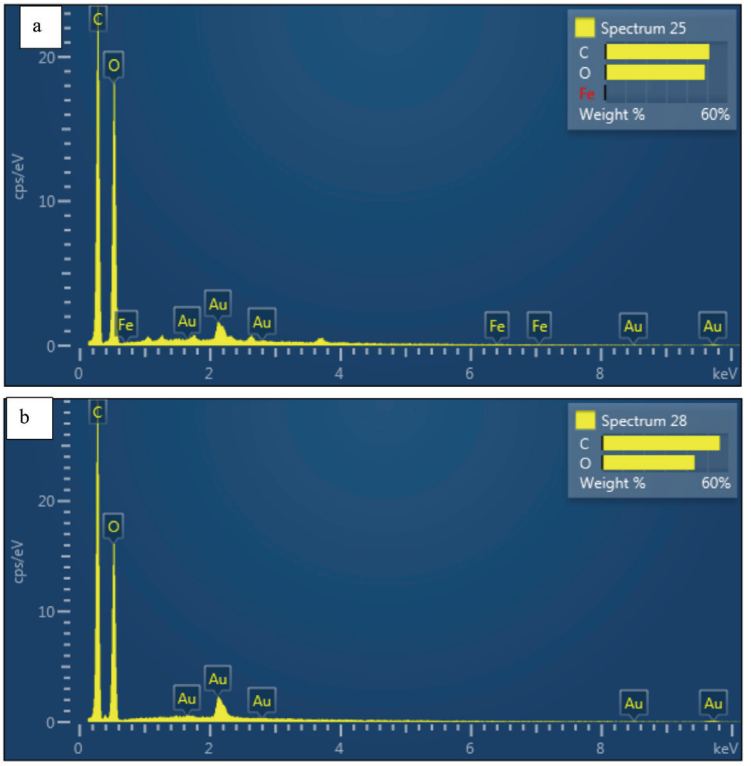

Figure 8: EDX of (a) CW and (b) NCW

Table 4: EDX for CW and NCW

Element	CW		NCW	
	Wt (%)	Atomic (%)	Wt (%)	Atomic (%)
C	51.02	58.16	55.97	62.87
O	48.86	41.81	44.03	41.81
Total	**100.00**	**100.00**	**100.00**	**100.00**

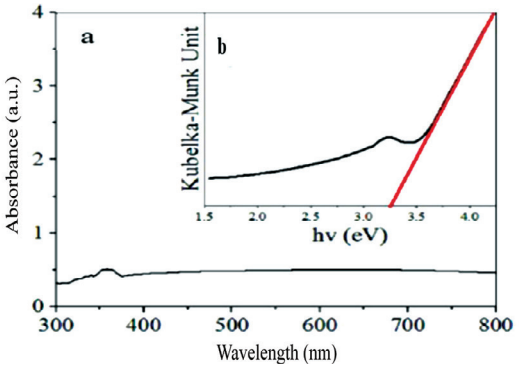

Figure 9: The analysis of (a) DRS and (b) the energy band gap

weight loss of 78% occurred as the sample was heated from 290°C to 385°C. Both of these losses were attributed to the presence of low molecular weight components and amorphous components within the NCWs. Overall, the NCWs samples exhibited relatively similar thermal characteristics compared to previously reported literature (Mohamed *et al*., 2021). These findings suggest that the thermal stability of NCWs extracted through ultrasound-assisted acid hydrolysis surpassed that of the raw materials, as indicated by comparisons with literature data (Wang & Lu, 2020).

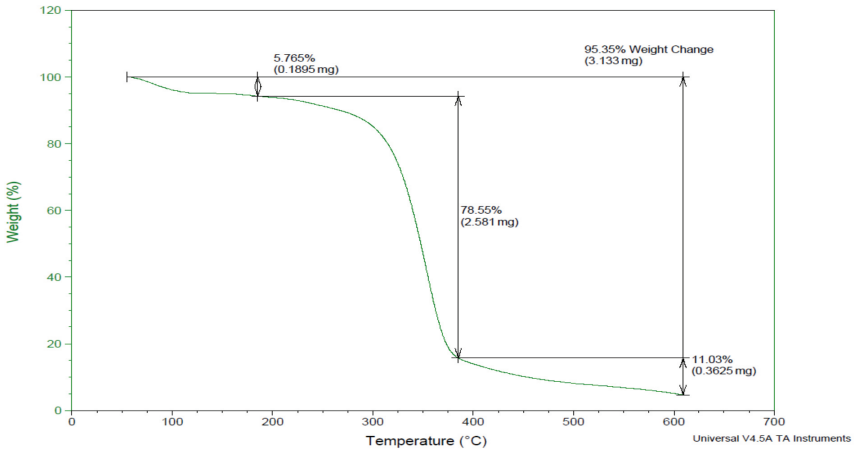

Figure 10: The TGA analysis for nanocellulose

Surface area and pore volume analysis of the prepared NCW sample were conducted using a BET device, revealing a surface area of 16.4 m^2/g in the present study. Notably, this BET surface area measurement exceeds the value that reported by Iqbal *et al*. (2022), suggesting potential differences in sample preparation, experimental conditions, or analytical techniques between studies as presented in Figure 11 (Pandi *et al*., 2021b).

Adsorption and Oxidation Treatment

The recovery of organic by way of function solar time, pH, nano dose, and Temperature of cellulose adsorption and oxidation are shown in equations (3) and (4) for NWC/solar, and NWC/UV respectively.

$$Y_{NCW/solar} = 19.7 + 0.215X_1 + 3.68X_2 + 11.9X_3 + 0.808X_4 - 0.000872X_1^2 - 0.171X_2^2 + 8.80X_3^2 - 0.00579X_4^2 + 0.0022X_1X_2 - 0.0543X_1X_3 + 0.00019X_1X_4 - 0.7X_2X_3 + 0.0043X_2X_4 - 0.155X_3X_4 \quad (3)$$

$$Y_{NCW/UV} = 40.7 + 0.126X_1 + 3.18X_2 + 2.7X_3 + 0.651X_4 - 0.000457X_1^2 - 0.182X_2^2 + 11.61X_3^2 - 0.00435X_4^2 + 0.0041X_1X_2 - 0.0615X_1X_3 + 0.00043X_1X_4 + 0.26X_2X_3 - 0.009X_2X_4 - 0.133X_3X_4 \quad (4)$$

where X1 is the solar time, X_2 is the pH, X_3 is the adsorbent dose and X4 is temperature.

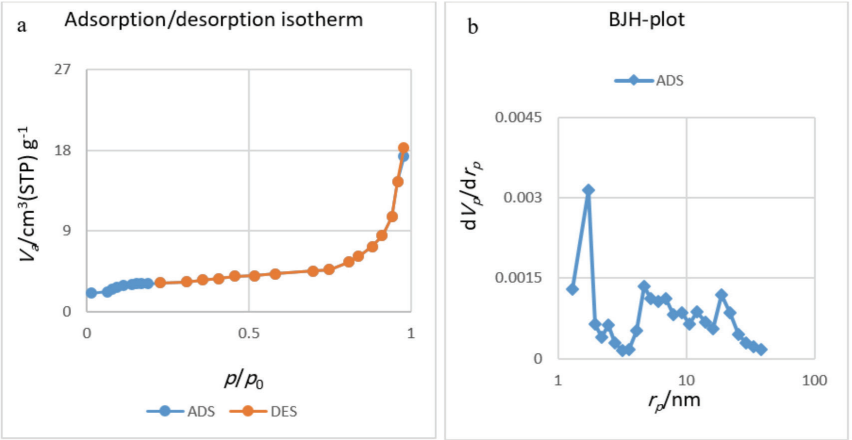

Figure 11: NCW of (a) ADS-DES isotherms and (b) BJH

The time effect on organic pollutants in wastewater using NCW under solar and UV light involves understanding the kinetics of adsorption and degradation processes and optimising treatment duration. The time required for significant degradation of organic pollutants depends on factors such as the intensity and duration of solar irradiation, pH, dose, and temperature, influencing the efficiency of the nanocellulose material in generating reactive species from solar and UV light and allowing for comparison between them. Experiments were conducted to find the best period for oxidation efficiency in the removal of organics in RWW (Naeem *et al*., 2018). With increased time useful for adsorption and oxidation, the elimination efficiency improved, as shown in Figure 12 (a). The oxidation of organic content by free radicals has been related to an increase in organic elimination competence.

The dose of NCW material significantly influences organic removal from RWW through adsorption and degradation under UV and solar light (Al-Zobai *et al*., 2020). Organic elimination increases quickly as the dose increases due to the availability of more functional groups in cellulose (OH), providing more exchangeable surface sites accessible to form complexes with organic pollutants, as depicted in Figure 12 (b).

pH significantly influences organic removal from RWW through adsorption and degradation using nanocellulose made from cotton waste by acid hydrolysis (Li *et al*., 2023). The highest adsorption and oxidation efficiencies were observed at a pH of 9, indicating significant improvement in organic removal, as shown in Figure 12 (c).

The influence of temperature on organic removal from RWW through adsorption and degradation by NCW made from cotton waste

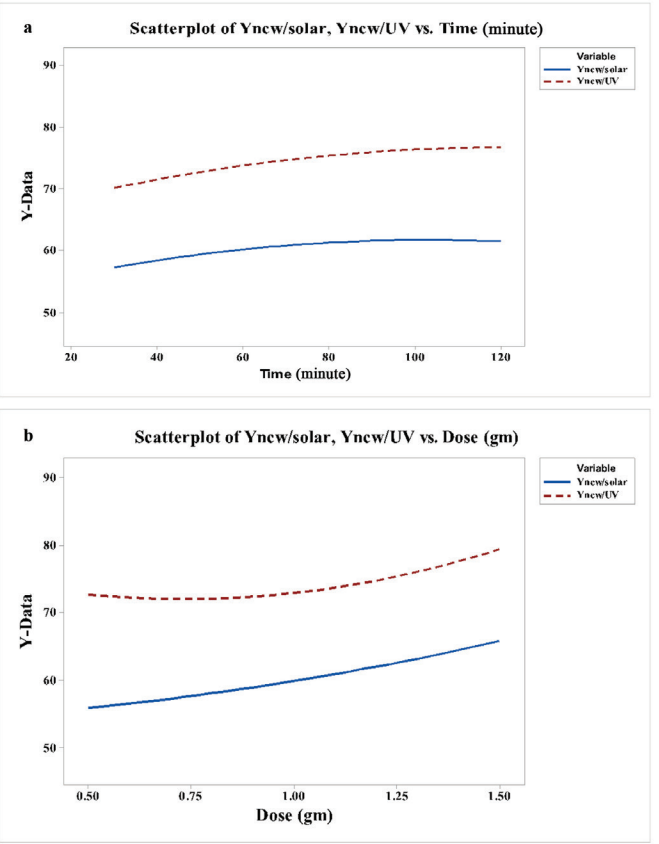

can vary depending on several factors. Increasing temperature can enhance adsorption kinetics and degradation processes by increasing the rate of reactions involved (Peralta-Hernández *et al*., 2018). However, excessively high temperatures might also cause degradation of the NCW material itself, affecting its efficiency. Increasing the temperature from 25°C to 70°C resulted in increased elimination of organics, as shown in Figure 12 (d). The effect of time on organic pollutants in wastewater using NCW under solar and UV light involves the kinetics of adsorption and degradation processes, optimising treatment duration (Hassan & Al-Zobai, 2019).

The plots illustrate the optimal combination of critical parameters for achieving the desired oxidation performance for NCW under UV and ultrasound, as depicted in Figure 13. Each plot showcases the optimal limits for specific performance metrics. Previous research has consistently indicated that organic elimination increases with higher levels of adsorbent dose, pH, temperature, and irradiation time (Nidheesh & Gandhimathi, 2012).

The results illustrated in Figure 14, indicate that the efficacy of elimination response increases with irradiation time during adsorption and oxidation for all organic pollutants for NCW under UV and solar light in Figure 12 (a) and (b), respectively. However, there is a tendency for a decline at a certain point due to insufficient surface area on the oxidation material, hindering the achievement of a relatively high elimination ratio (Jorgetto *et al*., 2014).

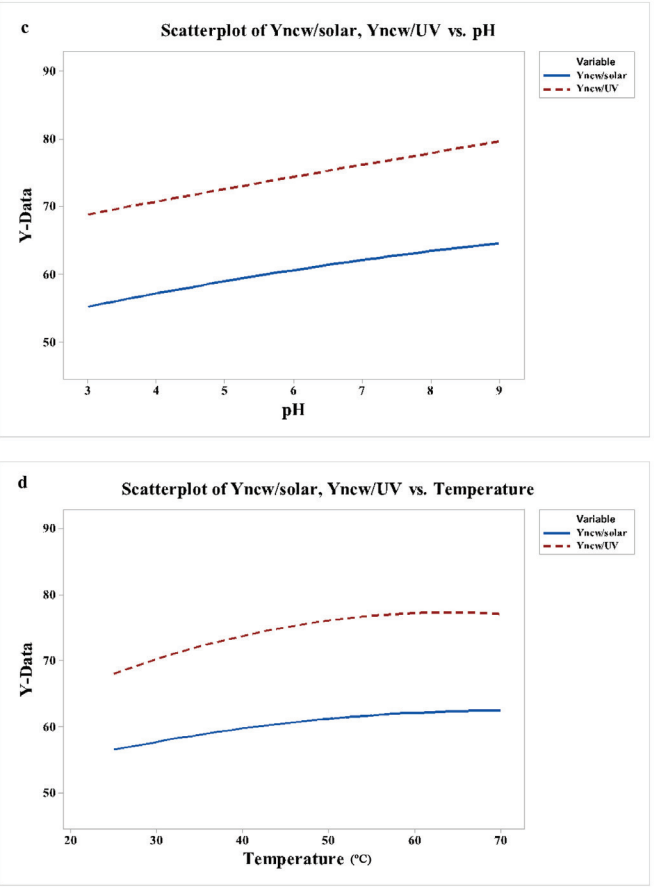

Figure 12: Effect of (a) time, (b) dose, (c) pH, and (d) temperature on RWW treatment

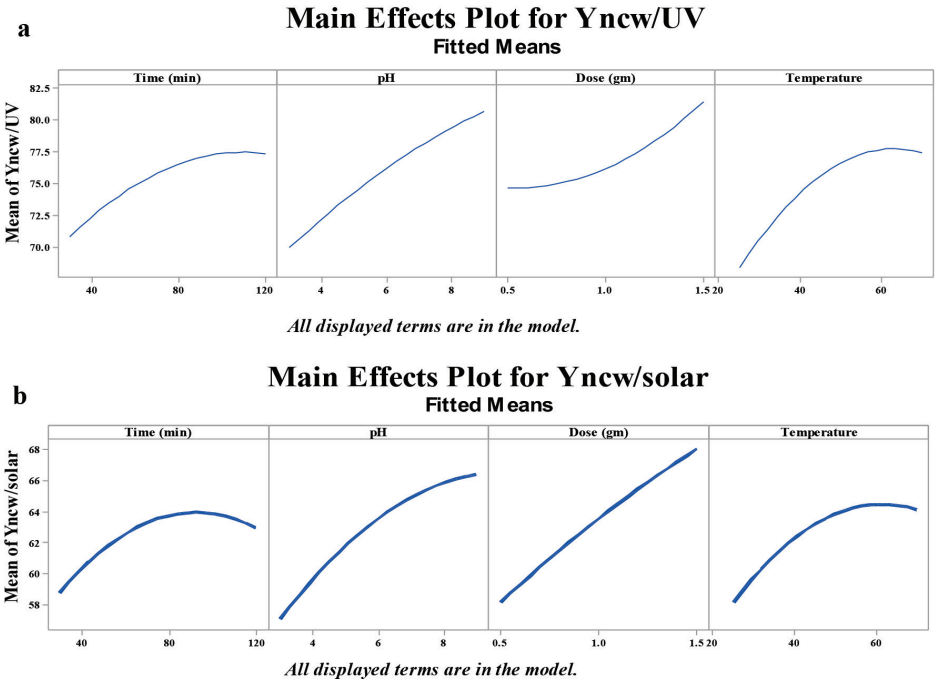

Figure 13: Main effects plot of NCW (a) UV light and (b) solar light

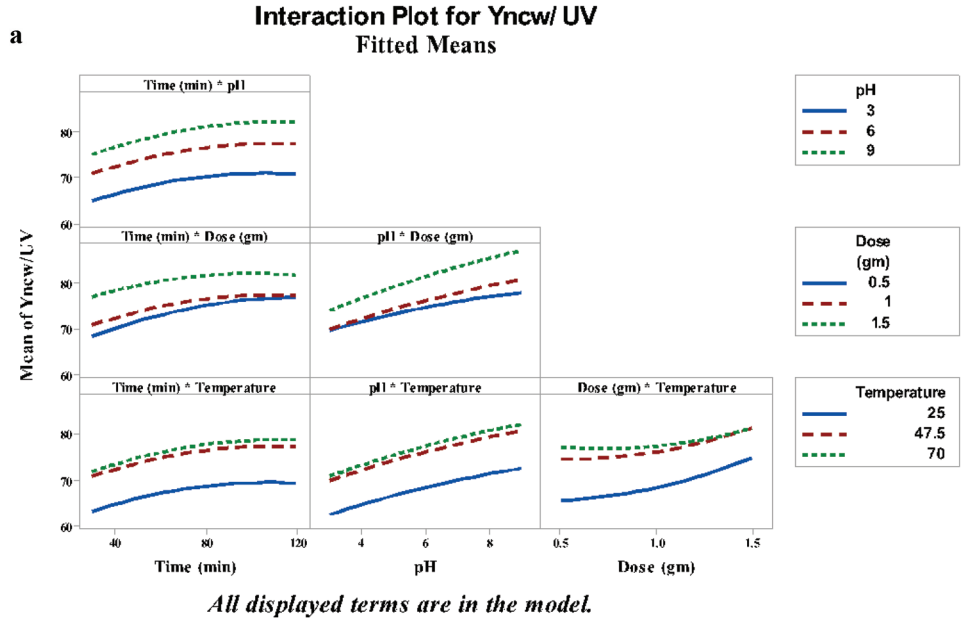

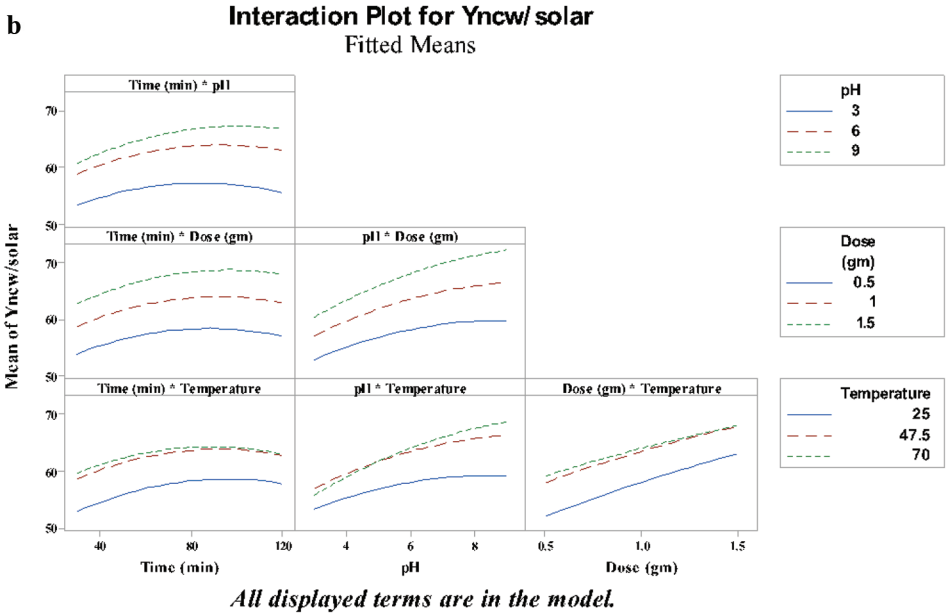

Figure 14: Interaction plot of (a) CW and (b) NCW

Enhancing Operational Efficiency through Parameter Optimisation

The optimal experimental conditions for treating refinery wastewater through adsorption and degradation were determined to achieve the best values for key parameters such as NCW dose, pH, time, and temperature. The measurement implications of the D-optimisation are depicted in Figure 15. Under these optimised conditions, the highest organic removal efficiencies were observed, reaching 92.5% and 82.4% for NCW under UV light and solar irradiation, respectively. These results highlight the effectiveness of the proposed approach in efficiently removing organic pollutants from refinery wastewater, demonstrating its potential for practical application in wastewater treatment processes, and compared with similar works in Table 5.

The Kinetics of Oxidation

The kinetics of the organic adsorption process onto NCW were investigated using pseudo-first-order and pseudo-second-order kinetic models. The pseudo-second-order kinetics equation was found to provide a better fit compared to the pseudo-first-order equation. Linear plots were obtained with the pseudo-first-order kinetics equation. Figure 16 illustrates the linearised form of the pseudo-second-order model (Ln (C_t/C_o) vs. time) with changes in NCW dose and pH, highlighting the important effects of these parameters on adsorption and photodegradation to remove organic pollutants from RWW. The effect of NCW dose addition on the photodegradation of organic pollutants under UV light increased free radicals and active sites.

The adsorbent was investigated under 50 minutes reaction time and 30°C temperature under eight UV light sources. The results indicated that the degradation rate increased with higher pH and NCW dose, leading to the generation of more hydroxyl radicals, facilitating the oxidation of organic pollutants, and promoting the reaction. However, the increase in organic degradation was relatively modest with the removal efficiency rising from 75.4% to 86% when the pH and NCW dose

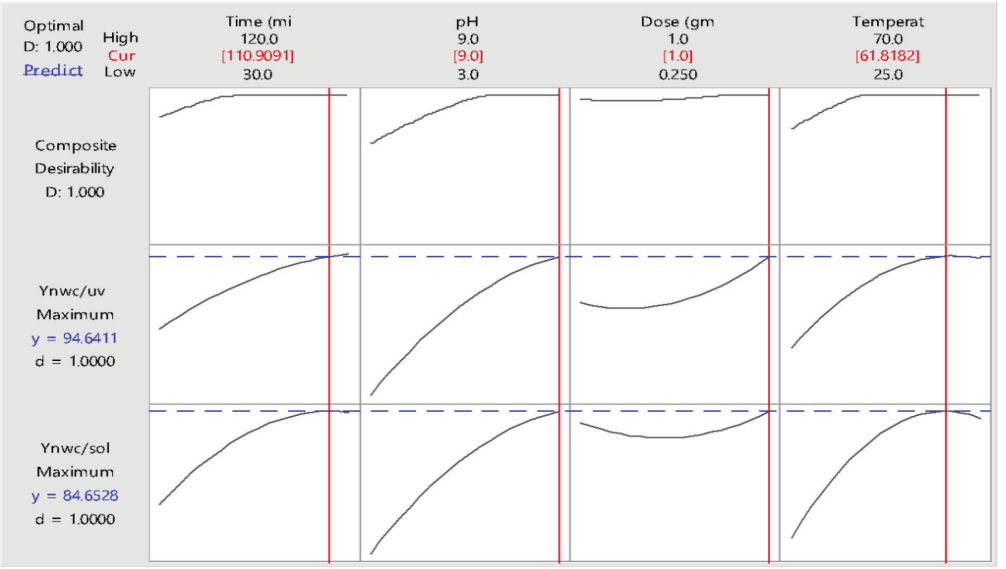

Figure 15: Finest employed variables for NCW

Table 5: Comparison between the prepared composite with other composites for treatment

Photocatalyst	Organic Pollutants	Irradiation Type	Time (minute)	Efficiency of Degradation (%)	References
ZnO/GO/ nanocellulose	Antibiotic	UV	120	98	Anirudhan and Deepa (2017)
Nanocellulose	Diclofenac	UV	120	82.4	Che Su *et al.* (2023)
Ag3PO4/NC composite	Methylene blue	UV	120	90	Lebogang *et al.* (2019)
NCW	OP	UV	120	92.5	This work

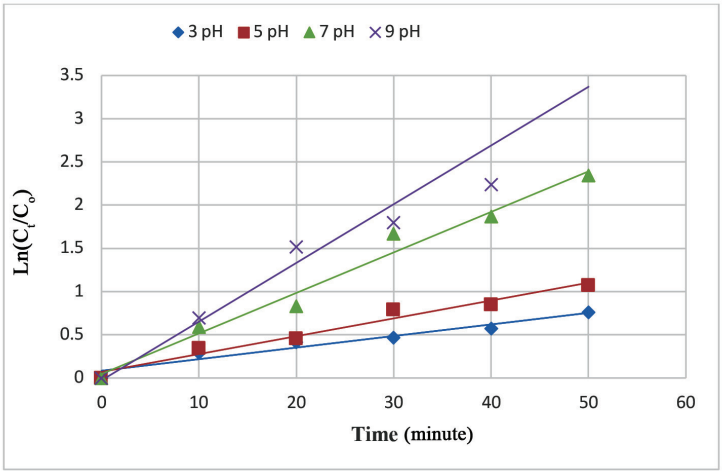

Figure 16: Plot of –Ln (C_t/C_o) of (a) pH and (b) NCW vs. time

were increased from 3 gm and 0.25 gm to 9 gm and 1 gm, respectively. Organic removal in wastewater involves complex reactions, making it challenging to differentiate individual reactions. Therefore, estimated kinetics for the degradation of organic solutions can be assumed with many researchers reporting that most organic elimination curves adhere to first-order or second-order kinetics (S. Raheem *et al*., 2024). The model of the first order is expressed as:

$$Ln\,(C_o/C_t) = K_1 t \quad (5)$$

where:

C_o, C_t = the initial concentration of organic mg/L (before and after treatment)

t = the time in minutes

K_1 = the first-order rate constant (min^{-1})

The degradation mechanism of organic pollutants over the NCW involves several steps, each facilitated by specific constituents within the heterostructure. When exposed to UV or solar light with energy equal to or greater than its band gap energy (3.2 eV) as shown in Figure 9 (b), the photogenerated NCW becomes photo excited, generating electron-hole pairs (e_{CB}- and h_{VB}+), illustrated in Figure 17. This process is described by Equation (6).

$$NCW + hv\ (visible\ light) \rightarrow NCW\ (e^- + h^+) \quad (6)$$

The preparation of NCW plays a crucial role in the degradation mechanism due to the increase in free radicals that remove organic pollutants and convert them to H_2O and CO_2. They create an electric field and a difference in band energy potentials, facilitating the migration of photogenerated electrons from VB to CB (Al-Jubouri *et al*., 2023). Photogenerated electrons react with oxygen molecules (O_2^-) to form oxygen radicals ($O_2^{\bullet-}$), as depicted in Equation (8) while holes react with adsorbed water and hydroxide ions (OH^-) to form hydroxyl radicals (•OH), as shown in Equations (7) to (9).

$$H_2O + h_{VB}^+ \rightarrow^{\bullet} OH + H^+ \quad (7)$$

$$O_2 + e_{CB}^- \rightarrow O_2^{\bullet-} \quad (8)$$

$$O_2^{\bullet-} + H_2O \rightarrow^{\bullet} OH + OH^- + O_2 + HO_2^- \quad (9)$$

Additionally, electron-hole pairs can directly oxidise organic molecules. The generated reactive oxygen species, including oxygen radicals and hydroxyl radicals, along with the direct oxidation by holes, facilitate the degradation of organic content present in the system. Figure 17 illustrates these steps visually, showing the migration of electrons and electron-hole pairs, the formation of reactive oxygen species, and the subsequent degradation of organic content over the photocatalyst under visible light irradiation (Somwanshi *et al*., 2020).

Conclusions

Because of the increasing amount of wastewater produced in the crude oil and gas industry, the release of polluted wastewater has become a significant ecological problem. In the meantime,

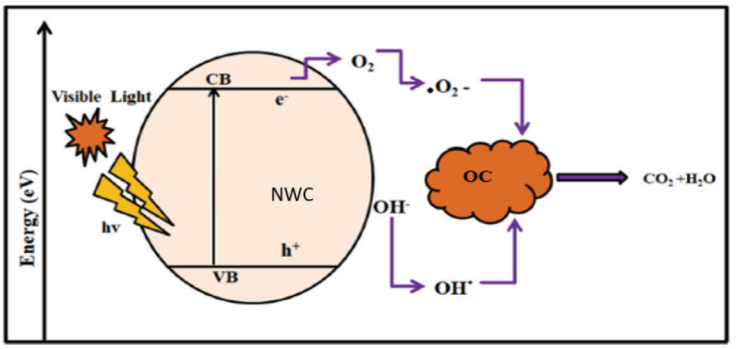

Figure 17: The possible mechanism of photodegradation

a single method of treatment is usually not adequate to eliminate all contaminants. The preparation of nanocellulose provides an efficient and low-cost material with high surface area and rich in functional groups compared to lignin and chitosan, offering a contamination-free choice for wastewater treatment in the oilfields industry. NCW was effectively manufactured employing combined acid hydrolysis with ultrasound under UV light. The results show that the ultrasound and light irradiation-assisted acid hydrolysis action was a well-organised method for the preparation of NCW from CW. The functional groups, the structural properties, and the morphology of the NCW were found to be effective for this purpose. It is expected that NCW will have promising requests in the field of wastewater treatment.

Acknowledgements

The authors would like to thank all reviewers for their comments and suggestions for the improvement of this article.

Conflict of Interest Statement

The authors declare that they have no conflict of interest.

References

Abdullah, R., Astira, D., Zulfiani, U., Widyanto, A. R., Hidayat, A. R. P., Sulistiono, D. O., Rahmawati, Z., Gunawan, T., Kusumawati, Y., Othman, M. H. D., & Fansuri, H. (2024). Fabrication of composite membrane with microcrystalline cellulose from lignocellulosic biomass as filler on cellulose acetate based membrane for water containing methylene blue treatment. *Bioresource Technology Reports*, *25*, 101728. https://doi.org/10.1016/j.biteb. 2023.101728

Alamery, H. R. D., & Ali, A. H. (2022). Effect of intensity of light and distance for decolonisation in direct red wastewater by photo fenton oxidation. *ARPN Journal of Engineering and Applied Sciences*, *17*(1819-6608), Article 9. https://www.arpnjournals.org/jeas/research_papers/rp_2022/jeas_0422_8910.pdf

Alfattal, A. H., & Ammar, S. A. (2019). Synthesized 2nd generation zeolite as an acid-catalyst for esterification reaction. *Iraqi Journal of Chemical and Petroleum Engineering*, *20*(3), 67-73. https://doi.org/10.31699/IJCPE.2019.3.9.

AlJaberi, F. Y., Basma A. A., Ali A. H., & Muhib L. G. (2020). Assessment of an electrocoagulation reactor for the removal of oil content and turbidity from real oily wastewater using response surface method. *Recent Innovations in Chemical Engineering (Formerly Recent Patents on Chemical Engineering)*, *13*(1), 55-71. https://doi.org/10.2174/2405520412666190830091842

Al-Jubouri, & Sama, M. (2019). The static aging effect on the seedless synthesis of different ranges FAU-type zeolite Y at various factors. *Iraqi Journal of Chemical and Petroleum Engineering*, *20*(4), 7-13. https://doi.org/10.31699/IJCPE.2019.4.2

Al-Jubouri, Sama, M., Huda Adil Sabbar, Hamzah A. L., & Basma I. Waisi. (2019). Effect of synthesis parameters on the formation 4a zeolite crystals: Characterisation analysis and heavy metals uptake performance study for water treatment. *Desalination and Water Treatment*, *165*, 290-300. https://doi.org/https://doi.org/ 10.5004/dwt.2019.24566

Al-Jubouri, S. M., Sabbar, H. A., Khudhair, E. M., Ammar, S. H., Batty, S. A., Khudhair, S. Y., & Mahdi, A. S. (2023). Chemistry silver oxide-zeolite for removal of an emerging contaminant by simultaneous adsorption-photocatalytic degradation under simulated sunlight irradiation. *Journal of Photochemistry and Photobiology*, *A: Chemistry*, *442*(March), 114763. https://doi.org/10.1016/j.jphotochem.2023.114763

Al-Zobai, K. M. M., Ali, A. H., & Nagam, O. K. (2020). Removal of amoxicillin from polluted water using UV/TiO_2, UV/

ZnO/TiO_2, and UV/ZnO. *Solid State Technology*, *63*(3), 3567-3575. http://solidstatetechnology.us/index.php/JSST/article/view/4489

Al-Zobai, K. M. M., & Hassan, A. A. (2022). Utilization of iron oxide nanoparticles (Hematite) as adsorbent for removal of organic pollutants in refinery wastewater. *Materials Science Forum*, *1065*, 91-100. https://doi.org/10.4028/p-i14w2f

Amelia, S. T. W., Adiningsih, S. N., Widiyastuti, W., Nurtono, T., Setyawan, H., Panatarani, C., Praseptiangga, D., Nazir, N., & Syamani, F. A. (2024). Novel cross-linking of toxic-free biopolymers for cellulose-gelatin films from avocado seed waste. *Bioresource Technology Reports*, *25*(November 2023), 101725. https://doi.org/10.1016/j.biteb.2023.101725

Anirudhan, T., & Deepa, J. (2017). Nano-zinc oxide incorporated graphene oxide/nanocellulose composite for the adsorption and photo catalytic degradation of ciprofloxacin hydrochloride from aqueous solutions. *Journal of Colloid and Interface Science*, *490*, 343-356. https://doi.org/10.1016/j.jcis.2016.11.042

Hassan, A., AlJaberi, F., & Al-Khateeb, R. (2022). Batch and continuous photo-fenton oxidation of reactive-red dye from wastewater. *Journal of Ecological Engineering*, *23*(1), 14-23. https://doi.org/10.12911/22998993/143864

Hassan, A. A., & Al-Zobai, K. M. M. (2019). Chemical oxidation for oil separation from oilfield produced water under UV irradiation using titanium dioxide as a nano-photocatalyst by batch and continuous techniques. *International Journal of Chemical Engineering*, *2019*, 1-8. https://doi.org/10.1155/2019/9810728

Ibrahim, Mohmad Khalel, Ali Abd Al-Hassan, & Ahmed Samir Naje. (2019). Utilisation of *Cassia surattensis* seeds as natural adsorbent for oil content removal in oilfield produced water. *Pertanika Journal of Science and Technology*, *27*(4), 2123-2138. http://www.pertanika2.upm.edu.my/resources/files/Pertanika%20PAPERS/JST%20Vol.%2027%20(4)%20Oct.%202019/38%20JST-1648-2019.pdf

Iqbal, D., Zhao, Y., Zhao, R., Russell, S. J., & Ning, X. (2022). A review on nanocellulose and superhydrophobic features for advanced water treatment. *Polymers*, *14*(12), Article 2343. https://doi.org/10.3390/polym14122343

Jayasinghe, J., Samarasekara, A., & Amarasinghe, D. (2020). Extraction of microfibrilated cellulose using waste garment cotton fabrics. *Tropical Agricultural Research*, *31*(2), Article 21. https://doi.org 10.4038/tar.v31i2.8364

Jorgetto, A., Silva, R., Saeki, M., Barbosa, R., Martines, M., Jorge, S., Silva, A., Schneider, J., & Castro, G. (2014). Cassava root husks powder as green adsorbent for the removal of Cu(II) from natural river water. *Applied Surface Science*, *288*, 356-362. http://dx.doi.org/10.1016/j.apsusc.2013.10.032

Kryeziu, A., Slovak, V., Parmentier, J., Zelenka, T., & Rigolet, S. (2022). Porous carbon monoliths from Ice-NaOH templated dissolved cellulose. *Industrial Crops and Products*, *183*, Article 114961. https://doi.org/10.1016/j.indcrop.2022.114961

Kurniawan, T. W., Sulistyarti, H., Rumhayati, B., & Sabarudin, A. (2023). Cellulose Nanocrystals (CNCs) and Cellulose Nanofibers (CNFs) as adsorbents of heavy metal ions. *Journal of Chemistry*, *2023*, 1-36. https://doi.org/10.1155/2023/5037027

Lebogang, L., Bosigo, R., Lefatshe, K., & Muiva, C. (2019). Ag_3PO_4/nanocellulose composite for effective sunlight driven photodegradation of organic dyes in wastewater. *Materials Chemistry and Physics*, *236*, Article 121756. https://doi.org/10.1016/j.matchemphys.2019.121756

Li, Y., Wu, Y., Chen, N., Ma, Y., Ji, W., & Sun, Y. (2023). Preparation of metal oxide-loaded nickel foam adsorbents modified by biochar

for the removal of cationic dyes from wastewater. *Chinese Journal of Analytical Chemistry*, *51*(8), Article 100278. https://doi.org/10.1016/j.cjac.2023.100278

Liu, P., Liu, L., Zhou, Z., Yuan, H., Zheng, T., Wu, Q., & Taoli, H. (2021). Insight into tar formation mechanism during catalytic pyrolysis of biomass over waste aluminum dross. *Applied Sciences (Switzerland)*, *11*(1), 1-15. https://doi.org/10.3390/app11010246

Mahmood, L. H., & Abid, M. F. (2020). Dmetallization of Iraqi crude oil by using zeolite A. *Indian Chemical Engineer*, *62*(1), 92-102. https://doi.org/10.1080/00194506.2019.1641432

Maiti, K., Thanh, T. D., Sharma, K., Hui, D., Kim, N. H., & Lee, J. H. (2017). Highly efficient adsorbent based on novel cotton flower-like porous boron nitride for organic pollutant removal. *Composites Part B Engineering*, *123*, 45-54. https://doi.org/10.1016/j.compositesb.2017.05.018

Meyabadi, T. F., Dadashian, F., Sadeghi, G. M. M., & Asl, H. E. Z. (2014). Spherical cellulose nanoparticles preparation from waste cotton using a green method. *Powder Technology*, *261*, 232-240. https://doi.org/10.1016/j.powtec.2014.04.039

Mhawesh, T. H., & Ali, Z. T. A. (2020). Reuse of brick waste as a cheap-sorbent for the removal of nickel ions from aqueous solutions. *Iraqi Journal of Chemical and Petroleum Engineering*, *21*(2), 15-23. https://doi.org/10.31699/ijcpe.2020.2.3

Mirzaei, M. (2021). Separation of oily pollution from water and wastewater by low cost and reusable composite based on natural fibers. *Advances in Environmental Technology 7*(2), 91-99. https://doi.org/10.22104/aet.2021.4906.1324

Mohamed, S. H., Hossain, M. S., Kassim, M. H. M., Ahmad, M. I., Omar, F. M., Balakrishnan, V., Zulkifli, M., & Yahaya, A. N. A. (2021). Recycling waste cotton cloths for the isolation of cellulose nanocrystals: A sustainable approach. *Polymers*, *13*(4), 1-17. https://doi.org/10.3390/polym13040626

Mohana, A. A., Rahman, M. A., Rahaman, M. H., Maniruzzaman, M., Farhad, S. M., Islam, M. M., Khan, M. S. I., & Parvez, M. Z. (2023). Okra Micro-Cellulose Crystal (MCC) and micro-clay composites for the remediation of Copper, Nickel, and Dye (Basic Yellow II) from wastewater. *Reactions*, *4*(3), 342-358. https://doi.org/10.3390/reactions4030021

Mondal, M. S., Paul, A., & Rhaman, M. (2023). Recycling of silver nanoparticles from electronic waste via green synthesis and application of AgNPs-chitosan based nanocomposite on textile material. *Scientific Reports*, *13*(1). https://doi.org/10.1038/s41598-023-40668-7

Motlagh, P. Y., Vahid, B., Akay, S., Kayan, B., Yoon, Y., & Khataee, A. (2023). Ultrasonic-assisted photocatalytic degradation of various organic contaminants using ZnO supported on a natural polymer of sporopollenin. *Ultrasonics Sonochemistry*, *98*, Article 106486. https://doi.org/10.1016/j.ultsonch.2023.106486

Naeem, H. T., Ali, A. H., & Raid, T. A. (2018). Wastewater-(Direct Red Dye) treatment-using solar fenton process. *Journal of Pharmaceutical Sciences and Research*, *10*(9), 2309-2313. https://www.researchgate.net/publication/328234109_Wastewater-Direct_red_dye_treatment-using_solar_fenton_process

Naser, G. F., Dakhil, I., & Hasan, A. (2021). Organic pollutants removal from oilfield produced water using nano magnetite as adsorbent. *Global NEST Journal*, *23*(3), 381-387. https://doi.org/10.30955/gnj.003875

Nawaf, A. T., Hamed, H. H., Hameed, S. A., Jarullah, A. T., Abdulateef, L. T., & Mujtaba, I. M. (2020). Performance enhancement of adsorption desulfurization process via

different new nano-catalysts using digital baffle batch reactor and mathematical modeling. *Chemical Engineering Science*, *232*, Article 116384. https://doi.org/10.1016/j.ces.2020.116384

Nawaf, A. T., Humadi, J. I., Jarullah, A. T., Ahmed, M. A., Hameed, S. A., & Mujtaba, I. M. (2023). Design of nano-catalyst for removal of phenolic compounds from wastewater by oxidation using modified digital basket baffle batch reactor: Experiments and modeling. *Processes*, *11*(7), Article 1990. https://doi.org/10.3390/pr11071990

Nawaf, A. T., Jarullah, A. T., & Abdulateef, L. T. (2018). Design of a Synthetic Zinc Oxide Catalyst over Nano-alumina for Sulfur Removal by Air in a Batch Reactor. *Bulletin of Chemical Reaction Engineering and Catalysis*, *14*(1), 79-92. https://doi.org/10.9767/bcrec.14.1.2507.79-92

Négrier, M., Ahmar, E. E., Sescousse, R., Sauceau, M., & Budtova, T. (2023). Upcycling of textile waste into high added value cellulose porous materials, aerogels, and cryogels. *RSC Sustainability*, *1*(2), 335-345. https://doi.org/10.1039/d2su00084a

Nidheesh, P., & Gandhimathi, R. (2012). Trends in electro-Fenton process for water and wastewater treatment: An overview. *Desalination*, *299*, 1-15. https://doi.org/10.1016/j.desal.2012.05.011

Nsaif, R. D., Alturki, S. F., Suwaed, M. S., & Hassan, A. A. (2023). Lead removal from refinery wastewater by using photovoltaic electro Fenton oxidation. *AIP Conference Proceedings*, *2876*, Article 050008. https://doi.org/10.1063/5.0163378

Pandi, N., Sonawane, S. H., & Kishore, K. A. (2021a). Synthesis of cellulose nanocrystals (CNCs) from cotton using ultrasound-assisted acid hydrolysis. *Ultrasonics Sonochemistry*, *70*, Article 105353. https://doi.org/10.1016/j.ultsonch.2020.105353

Pandi, N., Sonawane, S. H., & Kishore, K. A. (2020b). Synthesis of cellulose nanocrystals (CNCs) from cotton using ultrasound-assisted acid hydrolysis. *Ultrasonics Sonochemistry*, *70*, Article 105353. https://doi.org/10.1016/j.ultsonch.2020.105353

Peralta-Hernández, J. M., Vijay, S., Rodríguez-Narváez, O., & Pacheco-Álvarez, M. A. (2018). Photo and solar fenton processes for wastewater treatment. In *Electrochemical water and wastewater treatment* (pp. 223-237). https://doi.org/10.1016/b978-0-12-813160-2.00009-2

Qureshi, U., Hameed, B., & Ahmed, M. (2020). Adsorption of endocrine disrupting compounds and other emerging contaminants using lignocellulosic biomass-derived porous carbons: A review. *Journal of Water Process Engineering*, *38*, Article 101380. https://doi.org/10.1016/j.jwpe.2020.101380

Raheem, N. A., Majeed, N. S., & Timimi, Z. A. (2024). Phenol adsorption from simulated wastewater using activated spent tea leaves. *Iraqi Journal of Chemical and Petroleum Engineering*, *25*(1), 95-102. https://doi.org/10.31699/ijcpe.2024.1.9

Raheem, S., Al-Yaqoobi, A., Znad, H., & Abid, H. R. (2024). Caffeine extraction from spent coffee grounds by solid-liquid and ultrasound-assisted extraction: Kinetic and thermodynamic study. *Iraqi Journal of Chemical and Petroleum Engineering*, *25*(1), 49-57. https://doi.org/10.31699/ijcpe.2024.1.5

Rashid, A. H., Ali, A. H., Raid, T. H., & Naje, A. S. (2020). Treatment of oil content in oilfield produced water using chemically modified waste sawdust as biosorbent. *Ecology, Environment and Conservation*, *26*(4), 1563-1571. https://doi.org/10.1088/1742-6596/1294/7/072013

Shi, R., Wang, T., Lang, J., Zhou, N., & Ma, M. (2022). Multifunctional cellulose and Cellulose-based (NANO) composite adsorbents. *Frontiers in Bioengineering and Biotechnology*, *10*, Article 891034. https://doi.org/10.3389/fbioe.2022.891034

Simayee, M., Zad, A. I., & Esfandiar, A. (2023). Green synthesize of copper nanoparticles on the cotton fabric as a self-regenerating and high-efficient plasmonic solar evaporator. *Scientific Reports*, *13*(1), Article 12762. https://doi.org/10.1038/s41598-023-40060-5

Somwanshi, S. B., Somvanshi, S. B., & Kharat, P. B. (2020). Nanocatalyst: A brief review on synthesis to applications. *Journal of Physics Conference Series*, *1644*(1), Article 012046. https://doi.org/10.1088/1742-6596/1644/1/012046

Su, N. C., Basirun, A. A., Sultan, N. S. H., Kanakaraju, D., & Wilfred, C. D. (2023). Modified nanocellulose-based adsorbent from sago waste for diclofenac removal. *Sustainability (Switzerland)*, *15*(7), Article 5650. https://doi.org/10.3390/su15075650

Tan, W. Y., Gopinath, S. C. B., Anbu, P., Velusamy, P., Gunny, A. a. N., Chen, Y., & Subramaniam, S. (2023). Generation of microcrystalline cellulose from cotton waste and its properties. *BioResources*, *18*(3), 4884-4896. https://doi.org/10.15376/biores.18.3.4884-4896

Theivasanthi, T., Christma, F. A., Toyin, A. J., Gopinath, S. C., & Ravichandran, R. (2017). Synthesis and characterization of cotton fiber-based nanocellulose. *International Journal of Biological Macromolecules*, *109*, 832-836. https://doi.org/10.1016/j.ijbiomac.2017.11.054

Wang, Y., & Lu, Q. (2019). Dendrimer functionalized nanocrystalline cellulose for Cu(II) removal. *Cellulose*, *27*(4), 2173-2187. https://doi.org/10.1007/s10570-019-02919-7

Yu, X., Jiang, Y., Wu, Q., Wei, Z., Lin, X., & Chen, Y. (2021). Preparation and characterisation of cellulose nanocrystal extraction from pennisetum hydridum fertilized by municipal sewage sludge via sulfuric acid hydrolysis. *Frontiers in Energy Research*, *9*(November), 1-10. https://doi.org/1 10.3389/fenrg.2021.774783

Zang, N., & Qian, X. (2012). Influence of organic acid on thermal hazard of hydrogen peroxide. *Procedia Engineering*, *45*, 526-532. https://doi.org/10.1016/j.proeng.2012.08.198